Research Article

Hans Lochbihler*

Polarizing and angle-sensitive color filter in transmittance for security feature applications

Abstract: Subwavelength gratings comprising a stack of two thin metallic wire gratings embedded in a dielectric exhibit distinctive color properties in transmittance. Its angle-dependent coloring can be easily noticed by human observers in ambient light. Moreover, it has pronounced polarizing properties in the visible wavelength range. The optical properties of these gratings have been numerically studied. The results have been confirmed by manufactured samples replicated by a simple nanoimprint process on plastic foils. The manufacturing process is predestined for industrial mass production. Applications as authentication devices are given.

Keywords: authentication devices; coloring; subwavelength gratings.

OCIS codes: 050.6624; 330.1690.

DOI 10.1515/aot-2014-0056
Received November 4, 2014; accepted December 11, 2014; previously published online January 15, 2015

1 Introduction

The concept of color filtering by gratings in the zeroth diffraction is known since more than 30 years. Knop suggested phase gratings with deep rectangular grooves and periods <2 μm as color filters [1]. Recently, metallic subwavelength gratings have been proposed for color filtering in transmission [2–7]. Gratings comprising a thin continuous corrugated metallic film may exhibit colors in transmission arising from the excitation of surface plasmon-polaritons on the metal [3, 4].

Alternatively, metallic wire gratings can be used as color filters, if their profile is designed so that resonant light interaction occurs in the visible range [2]. Colored images may be manufactured by this kind of gratings having a lateral variable modulation depth. Moreover, stacked wire gratings have been developed for color filtering in transmittance [5–7]. The stack of wires forms microresonators and, subsequently, yields to distinct maxima in transmittance.

These structures exhibit a colored angle-sensitive transmission, and in addition, they have polarizing properties. Hence, their optical properties might be useful designing novel security labels for human observers. It is worth mentioning that alternative grating structures based on guided resonance filters were recently proposed for authentication labels [8].

However, apart from their visual appearance, security labels, especially for banknotes, have to fulfill further conditions: The effort for counterfeit must be very high, while its manufacturing costs must be cheap. Furthermore, the optical properties of a security label should not change under extreme environmental conditions. Its lifetime shall be beyond several years. We point out that only a few of proposed grating structures as color filters from the literature meet all of these constraints for designing novel security labels.

In this paper, the optical properties of a grating structure disclosed in [6] are numerically investigated. Then, the coloring has been evaluated from the calculated transmittance spectra for different angles of incidence as well as for different light polarizations. Next, we outline the manufacturing process and present transmittance spectra from fabricated grating samples. Finally, the visual appearance of a manufactured security label is demonstrated.

2 Optical properties of wire grating structure

The profile of the proposed grating structure is illustrated in Figure 1A. It comprises a stack of two identical metallic wire gratings with the parameters: Period d, wire width $b=d/2$, wire thickness t, and the optical constants of the

***Corresponding author: Hans Lochbihler,** Louisenthal GmbH, P.O. Box 1185, D-83701 Gmund, Germany,
e-mail: hans.lochbihler@louisenthal.com

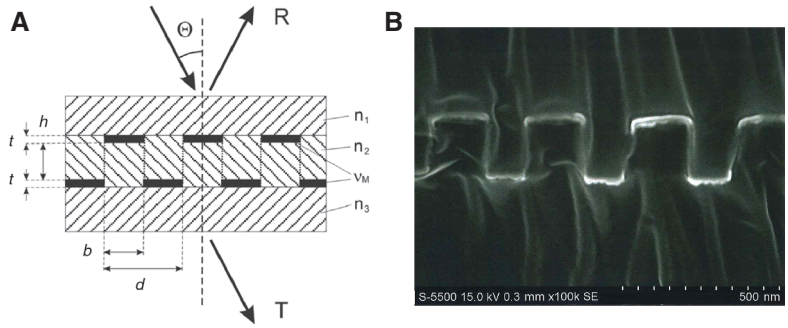

Figure 1 Profile of the presented grating structure with period *d*, width *b*, thickness of metallic films *t*, and distance between wire gratings *h*: sketch (A) and SEM image (B) of manufactured grating with *d*=360 nm, *h*=190 nm, and *t*=25 nm.

metallic stripes ν_M. The vertical distance between both wire gratings is defined by the parameter h. The wire gratings are horizontally shifted to each other by *d/2* and surrounded by a dielectric environment with refractive indices n_1, n_2, and n_3. The cross section of a manufactured grating replica represents the electron micrograph in Figure 1B. The wire structure consists of 25-nm-thick aluminum stripes, which are completely embedded in UV curable resin.

Now, the optical properties of this kind of gratings are investigated numerically. The parameters for the presented example are *d*=360 nm, *b*=180 nm, and $n_1=n_2=n_3=1.52$. Both metallic wire gratings consist of aluminum with thickness *t*=25 nm. The diffraction efficiencies have been calculated by means of a rigorous modal method with modal field expansions [9] and using the S-matrix method. For the numerical study, we used measured optical constants of aluminum. It is well known that the optical constants of thin metallic films deviate strongly from those of bulk materials. Hence, we measured these data for different aluminum films having thicknesses between 20 nm and 80 nm by means of a spectroscopic ellipsometer. For the numerical calculations using a specific thickness, the optical constants were interpolated from those measured data sets. As an example, the data for a film having a thickness of 25 nm is shown in the inset of Figure 2B, which also illustrates the deviation from the values for the bulk material [10].

The transmittance as a function of wavelength was calculated for unpolarized incident light at the angle Θ=0° and at angle Θ=30°. In the calculation, unpolarized incident light was treated as a superposition of transverse magnetic and transverse electric waves. The influence of the grating geometry to the transmission spectra is exemplified in Figure 2 by varying the distance *h* between 100 nm and 250 nm. Pronounced resonant maxima occur

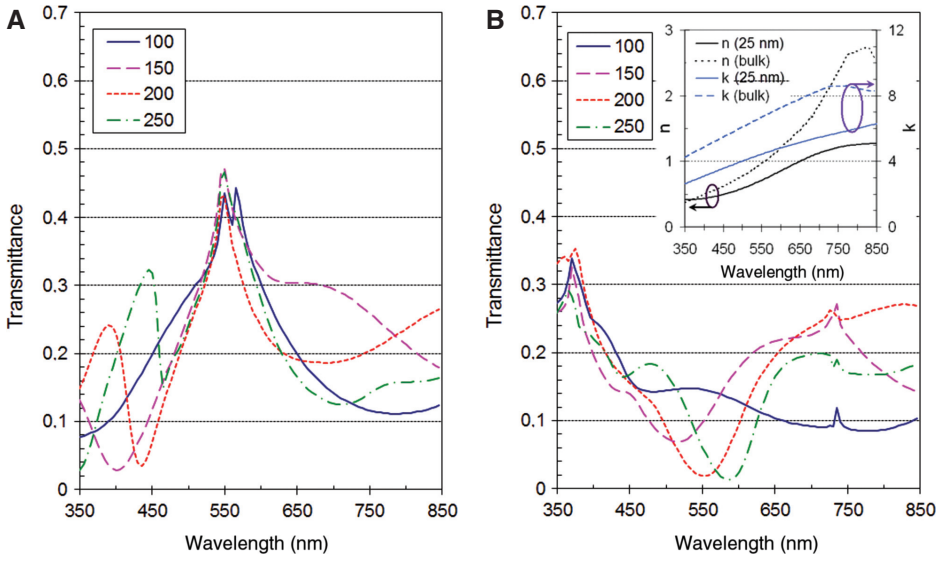

Figure 2 Calculated transmittance as a function of wavelength of grating (*d*=360 nm, *b*=180 nm, *t*=25 nm, n=1.52) for different distances *h*=100–250 nm and at (A) angle Θ=0° and (B) angle Θ=30° for unpolarized incident light.

for normal incidence at wavelength 548 nm, corresponding to the Rayleigh anomaly, where the first diffraction orders become evanescent.

A further resonant peak appears in the blue wavelength range for h=200 nm and h=250 nm.

Tilting the grating by Θ=30°, the resonance splits into two peaks located in the blue and in the red wavelength regions, respectively. Their positions can be easily estimated by means of the grating equation. In addition, a pronounced dip is formed at wavelength $\lambda\approx$550 nm for $h\geq$150 nm.

Then, the transmittance, the reflectance, and the power losses are analyzed for a grating with parameters from above, but for the fixed parameter h=200 nm. Figure 3 shows the spectra as a function of wavelength for unpolarized incident light at different angles Θ. For normal incidence, a distinct dip in transmittance lies at λ=435 nm, which is shifted to the longer wavelength regime for increasing angle of incidence. The corresponding peak in the power loss spectrum indicates that surface plasmon-polaritons are excited for these wavelengths [11]. Furthermore, it is worth noting that, on average, about 30% of incident light is absorbed in the visible wavelength regime.

How does the transverse magnetic and transverse electric waves contribute to these transmittance spectra? For that, the transmittance of the two fundamental cases of polarization is analyzed: TM polarization, when the E-vector of the impinging light oscillates perpendicular to the wires, and TE polarization, if the E-vector vibrates parallel to the wires. The transmittance curves for TE and TM polarization are presented in Figure 4. The grating parameters are the same as in Figure 3. It demonstrates that the grating greatly transmits TE-polarized light, and it strongly suppresses transmission for TM polarization. In addition, enhanced transmission of TE polarization occurs at normal incidence for wavelength $\lambda\approx$550 nm. Note that this peak is damped for increasing angle of incidence. This behavior of resonance appears rather similar as the resonant light transmission of thick wire gratings [12, 13]. The transmittance for TM polarization, however, is greatly damped due to the excitation of surface plasmon-polaritons [11].

It can be concluded from these transmission curves that these gratings act as efficient polarizers in the visible wavelength range. In addition, they exhibit distinct color-filtering properties. Moreover, the transmitted color strongly varies by the angle of incidence.

In order to quantify the color perception for a human observer, the chromaticity coordinates x and y were calculated from transmittance spectra with parameters given above as a function of angle Θ. In the algorithm, these spectra were convolved with the sensitivity of the human eye (10° observer) and the emissivity of the standard illuminant D65, which represents roughly the daylight spectrum [14]. Figure 5A shows the evaluated data as a trajectory in the chromaticity diagram of the CIE-1931 color space. Note that the hollow circle in the center of the diagram represents the white point. The continuous line marked by 'diamond' symbols represents the transmitted colors of unpolarized incident light by tilting the grating from normal incidence to the angle Θ=45°. It demonstrates a strong color change from yellow to blue, if the grating is tilted from normal incidence to about 30°. Furthermore, the

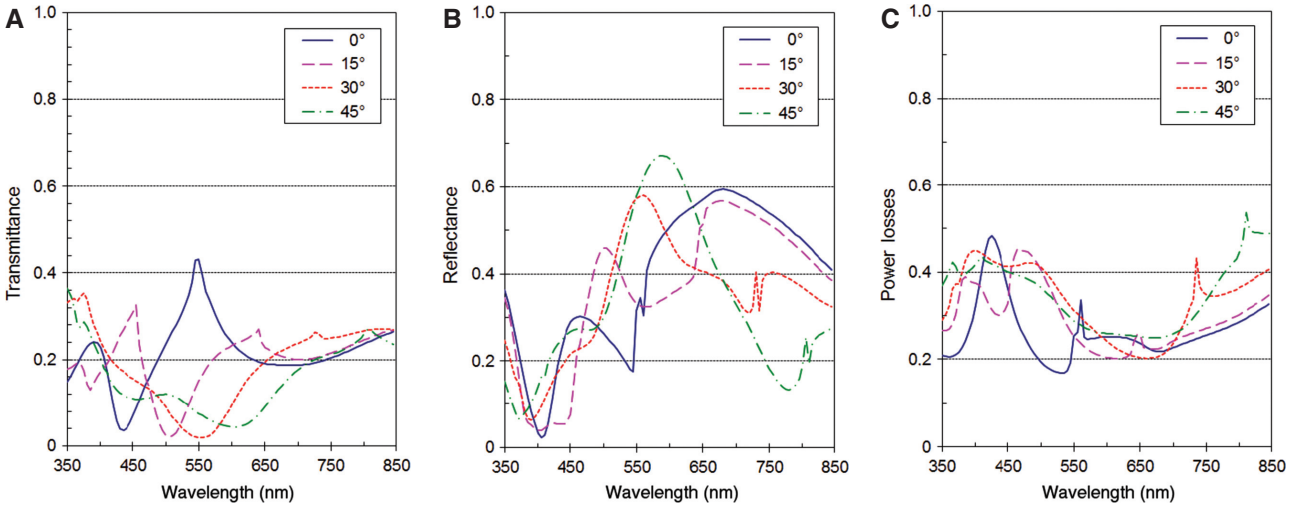

Figure 3 Calculated transmittance (A) reflectance (B) and power losses (C) of grating with parameters from Figure 2 and h=200 nm for different angles Θ=0°–45° at unpolarized incident light.

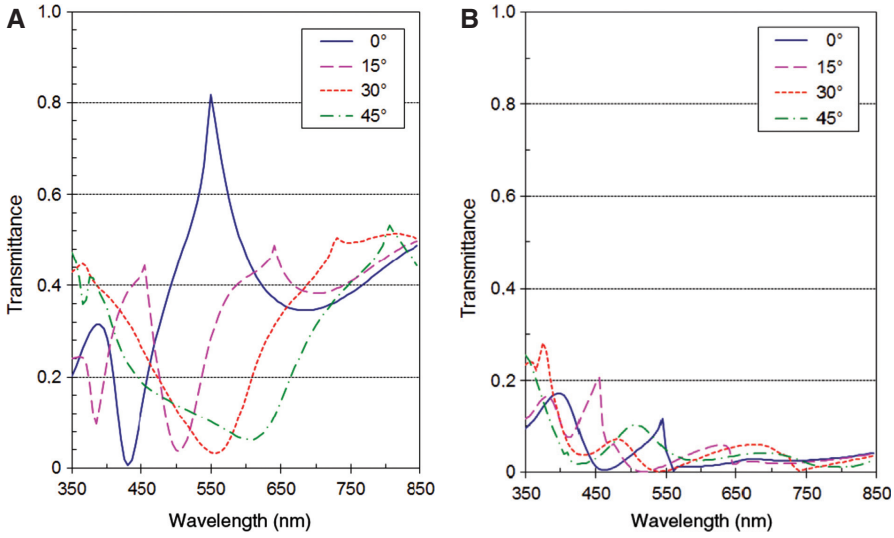

Figure 4 Calculated transmittance of grating from Figure 3 at different angles Θ=0°–45° for (A) TE-polarized and (B) TM-polarized incident light.

colors of polarized incident light are shown for the angles Θ=0° and Θ=30° by different symbols. It can be seen in the color space diagram that the colors for TE polarization lie close by the trajectory for unpolarized light. The colors for TM polarization, however, are different.

Moreover, we investigated the brightness of the colors using the *Lab* color space. Keep in mind that the CIE-1931 chromaticity diagram does not contain any brightness information of its colors. It also has to be emphasized that many applications of reproducing colors, especially for daylight conditions, demand a distinct lightness of the hue. The lightness L^* as a function of angle Θ is illustrated in Figure 5B for unpolarized light as well as for TE and TM polarization. The formulae for the calculation of L^* can be found in Ref. [14]. A lightness of $L^*=61$ occurs for unpolarized light at normal incidence. However, the lightness is reduced for increasing angle of incidence and has a minimum of 30 for Θ≈35°. For TE polarization, the lightness is even higher and has similar characteristics as unpolarized light. The lightness for TM polarization,

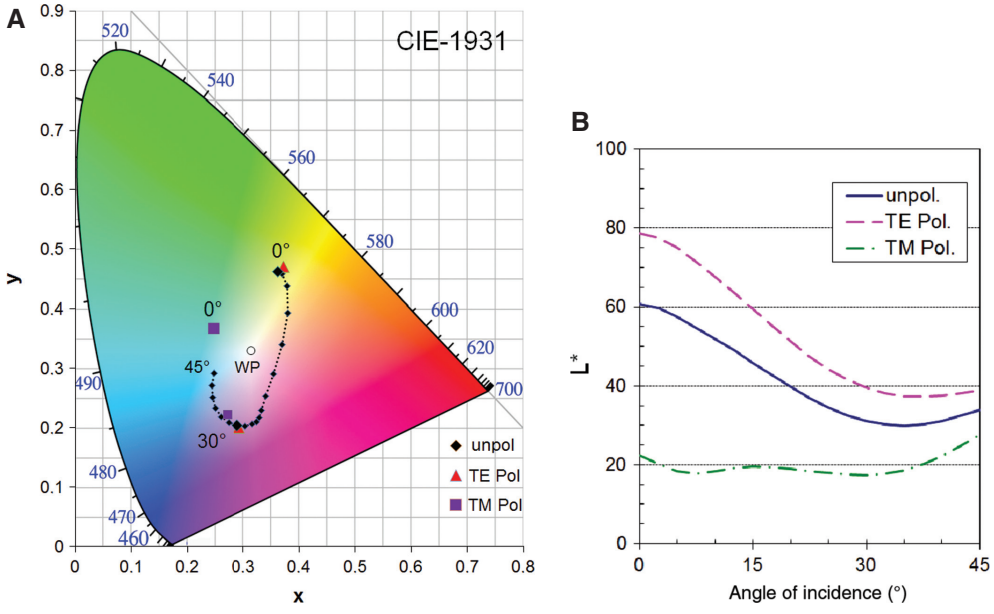

Figure 5 Transmitted colors of a grating with parameters from Figure 3 for different angles Θ=0°–45° as coordinates (*x*, *y*) in CIE-1931 chromaticity diagram (A) and lightness L^* for unpolarized as well as polarized incident light (B).

however, is significantly lower and almost constant for a variation of angle Θ. These results indicate that the hue of this kind of gratings may be easily noticed by a human observer under ambient light conditions.

3 Manufacturing

Having exemplified the coloring properties, we briefly illustrate the manufacturing of the grating structure and its subsequent replication process. First, a lamellar grating with homogeneous groove depth was fabricated by electron beam lithography (EBL) and transferred into a quartz master by an etching process. From this master, a Ni-mold is made by electroforming. The subsequent replication process is sketched in Figure 6.

After fabrication of the mold master, the lamellar grating is replicated in UV resin on, e.g., Polyethylenterephthalat (PET) foils or glass sheets. Note that the refractive indices of these materials are approximately 1.5. Subsequently, these replicas were coated with an aluminum layer of 25 nm on the top side by directional electron beam evaporation under high vacuum conditions. It is worth mentioning that metallic stripes are formed on the top and on the bottom of the rectangular grating profile. There is practically no sidewall deposition of aluminum in our evaporation process. Finally, the structure was filled with UV resin and covered on top by a thin dielectric superstrate, e.g., a PET foil. Ultimately, the grating structure comprising a stack of two thin aluminum wire gratings is formed, which are completely embedded in UV resin (also compare Figure 1B). We emphasize that this replication procedure is well suited to be implemented as a continuous roll-to-roll process, which is rather cost effective for mass production.

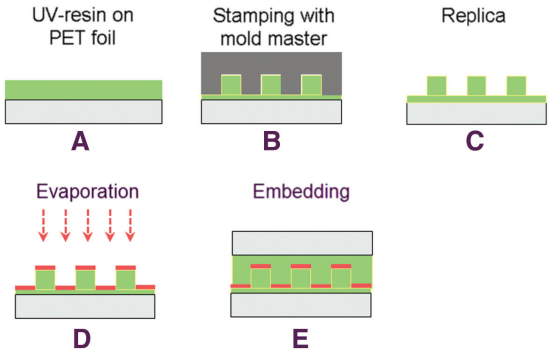

Figure 6 Replication process for grating structure: UV resin layer on PET foil (A), lamellar grating transferred from mold master (B), grating replica on PET foil (C), metallic coating (D), and embedding in UV resin (E).

Moreover, we have validated our numerical study by experimental data. The grating samples were manufactured as described above, each grating replica had a size of 20×20 mm. The transmittance was measured by a commercial spectrophotometer. This spectrometer, equipped with a depolarizer and narrow aperture stops, provides unpolarized light at an adjustable incidence angle Θ on the grating sample. Then, these data are compared with the calculated curves using the parameters d=360 nm, b=180 nm, h=220 nm, and $n_1=n_2=n_3=1.52$. The metallic wire gratings consist of aluminum with thickness t=25 nm. Figure 7 shows the measured and calculated transmittance curves in the visible wavelength region for unpolarized incident light at angles Θ=0° and Θ=30°.

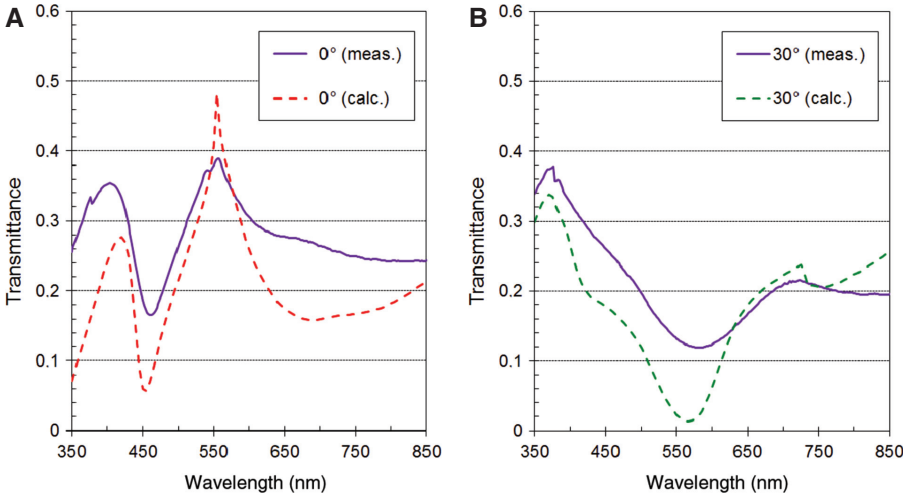

Figure 7 Measured and calculated transmittance as a function of wavelength for unpolarized incident light (A) at normal incidence and (B) at angle Θ=30°. The grating parameters for the calculation are d=360 nm, b=180 nm, h=220 nm, t=25 nm, n=1.54.

It demonstrates a good agreement between experimental and numerical data. The characteristics of resonant light transmission are fully confirmed by the experiment. Remaining discrepancies mainly arise from deviations of the wire cross section from the assumed rectangular profile and from slight birefringent properties of the PET substrate. Finally, it is worth mentioning that the color properties of this kind of gratings are only little affected by these imperfections.

In addition, the calculated transmittance for polarized incident light has been compared with experimental data. The transmittance of that grating replica from Figure 7 was measured for TE polarization as well as for TM polarization at normal incidence by means of a spectrophotometer equipped with Glan prisms. A comparison between measured and calculated data is presented in Figure 8. It was found that the positions of resonant peaks and dips agree well for both polarization cases. This validates our numerical model using the assumed grating profile and the grating parameters.

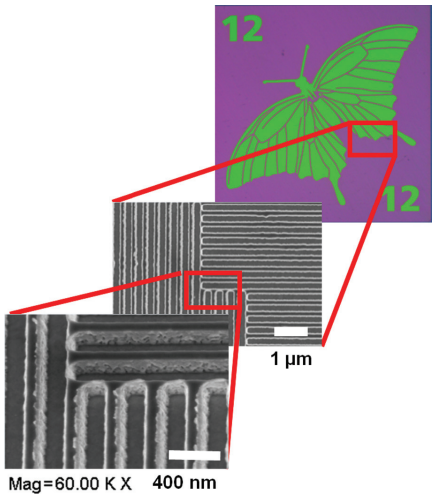

Figure 9 Image of manufactured security feature showing grating arrangement by SEM images.

4 Application as security labels

Having discussed the optical properties, we present now a design of a security label made of this kind of grating structure. Figure 9 shows an image from this label containing the motif 'butterfly' and the numbers '12' comprising the above-described grating. This image has been taken from a manufactured grating replica by a digital camera. The size of the sample was 10×10 mm. The grating inside the motif is horizontally oriented, whereas the grating forming the background is vertically oriented. This arrangement of gratings is illustrated by the SEM images taken from the mold master on the transition between motif and background.

We point out that these samples already have been manufactured by an industrialized mass-production process. The replication process as well the evaporation was performed by means of continuous roll-to-roll facilities. The paper of Ting et al. [15] provides an insight in this technique. We already achieved a high throughput and yield in production for this kind of structures.

Finally, a vivid impression of a manufactured security label is presented in Figure 10. It shows the coloring in transmittance from a sample taken with a conventional

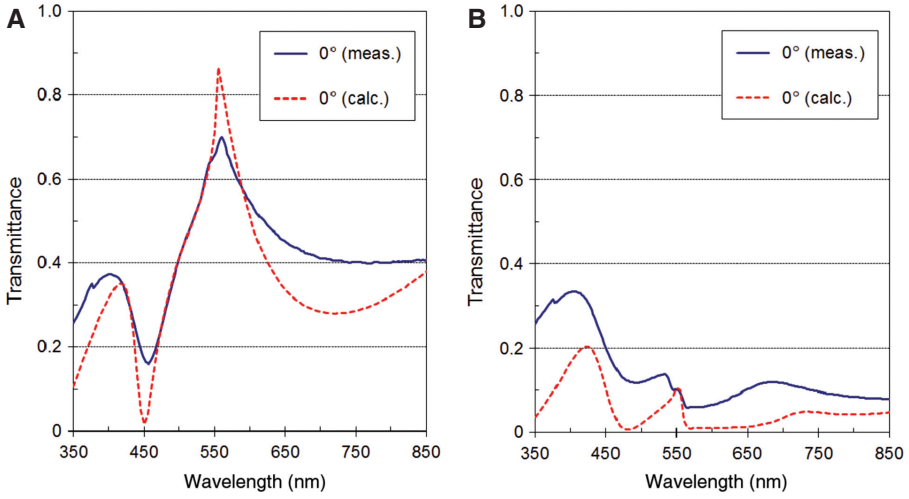

Figure 8 Measured and calculated transmittance as a function of wavelength for (A) TE-polarized and (B) TM-polarized light at normal incidence. The measured sample as well as the grating parameters for the calculation are the same as in Figure 7.

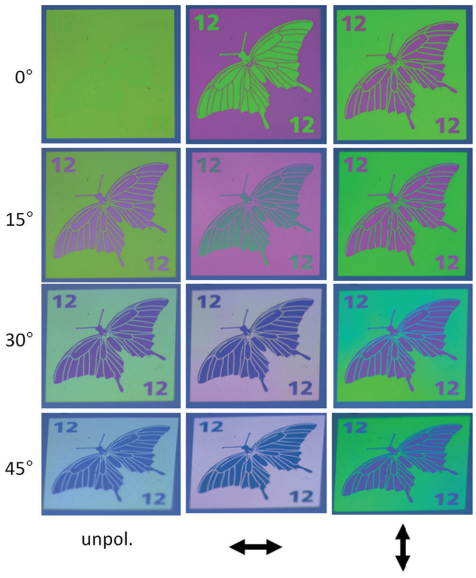

Figure 10 Visual appearance of manufactured sample at different angles Θ=0°–45° for unpolarized incident light and linear polarized light.

digital camera and illuminated by a light source with an emission spectrum equivalent to that of daylight. The coloring is shown for the angles of incidence Θ=0°, 15°, 30°, and 45°. These images have been taken for unpolarized incident light, as well as for linear polarized light (horizontally and vertically oriented relative to the sample).

The most surprising effect occurs for unpolarized incident light: An observer only perceives a homogeneous colored area for normal incidence. If the sample is slightly tilted by the horizontal axis, the motif appears instantaneous and has a strong magenta/blue coloring for the angle Θ=30°. The coloring of the background, however, only changes slightly by tilting the sample. Second, the colored motif is still present for linear polarized light at normal incidence. The colors of the motif and the background interchange, when the polarizer is turned, or if the sample is rotated by 90°. Moreover, the strong drop of lightness for increasing angle Θ supports the perception of the motif for inclined viewing.

5 Conclusions

The optical properties of subwavelength gratings comprising a stack of two thin metallic wire gratings embedded in a dielectric were investigated. This kind of gratings exhibit distinct resonances in transmittance. Hence, they may be used as efficient color filters in transmission. In addition, they have strong polarizing properties in the visible wavelength range. This provides that this kind of grating structure simultaneously acts as a color filter and a polarizer. Moreover, it was shown that the coloring and polarizing properties of manufactured samples agree well with the numerical predictions. Special attention was drawn to the fabrication process of these gratings. It was demonstrated that they can be replicated on plastic foils in large numbers by a cheap mass production process.

Finally, an example of a colored motif was presented which was formed by this kind of gratings having different grating orientations. A vivid impression of its visual appearance was given for different angles of incidence as well as for different states of light polarization. Because of its unique color properties, this kind of grating structures has promising applications as security labels.

Acknowledgments: I thank Professor Christian Lehmann from the Max-Planck-Institut fuer Kohlenforschung for the SEM analysis.

References

[1] K. Knop, Appl. Opt. 17, 3598–3603 (1978).
[2] H. Lochbihler, Opt. Exp. 17, 12189–12196 (2009).
[3] Y. Jourlin, S. Tonchev, A. V. Tishchenko, C. Pedri, C. Veillas, et al., Opt. Exp. 17, 12155–12166 (2009).
[4] V. Petiton, et al., WO2011/136777 A1, 8.4.2011.
[5] T. Xu, Y.-K. Wu, X. Luo and L. J. Guo, Nat. Commun. 59, 1–5 (2010).
[6] H. Lochbihler, WO2013/053435 A1, 11.10.2011.
[7] Z. Ye, J. Zheng, S. Sun, S. Chen and D. Liu, Plasmonics 8, 555–559 (2013).
[8] M.-L. Wu, C.-L. Hsu, H.-C. Lan, H.-I. Huang, Y.-C. Liu, et al., Opt. Lett. 32, 1614–1616 (2007).
[9] L. Li, J. Opt. Soc. Am. A 10, 2581–2591 (1993).
[10] E. D. Palik, 'Handbook of Optical Constants of Solids Part II' (Academic, New York, 1985).
[11] H. Lochbihler, Phys. Rev. B 50, 4795–4801 (1994).
[12] H. Lochbihler, Phys. Rev. B 79, 245427-8 (2009).
[13] C. Cheng, J. Chen, D.-J. Shi, Q.-Y. Wu, F.-F. Ren, et al., Phys. Rev. B, 78, 075406 (2008).
[14] G. A. Klein, 'Industrial Color Physics' (Springer, Berlin, 2010).
[15] C.-J. Ting, F.-Y. Chang, C.-F. Chen and C. P. Chou, J. Micromech. Microeng. 18, 075001 (2008).